Acta Crystallographica Section D
Biological Crystallography
ISSN 0907-4449

Structural flexibility, an essential component of the allosteric activation in *Escherichia coli* glucosamine-6-phosphate deaminase

E. Rudiño-Piñera,* S. Morales-Arrieta,† S. P. Rojas-Trejo and E. Horjales

Departamento de Reconocimiento Molecular y Bioestructura, Instituto de Biotecnología, Universidad Nacional Autónoma de Mexico, PO Box 510-3, Cuernavaca, MOR 62271, Mexico

† Present address: Centro de Investigaciones Biológicas del Noroeste, Mar Bermejo 195, La Paz, BCS 23090, Mexico.

Correspondence e-mail: rudino@ibt.unam.mx

Received 5 March 2001
Accepted 8 October 2001

PDB References: R form glucosamine-6-phosphate deaminase complex with fructose 6-phosphate at 2.15 Å, 1fqo; R form glucosamine-6-phosphate deaminase complex with *N*-acetylglucosamine-6-phosphate at 2.10 Å, 1frz; *R* form glucosamine-6-phosphate deaminase complex with *N*-acetylglucosamine-6 phosphate at 1.73 Å, 1fs5; T form glucosamine-6-phosphate deaminase at 2.2 Å, 1fs6; T form glucosamine-6-phosphate deaminase at 1.9 Å, 1fsf.

A new crystallographic structure of the free active-site R conformer of the allosteric enzyme glucosamine-6-phosphate deaminase from *Escherichia coli*, coupled with previously reported structures of the T and R conformers, generates a detailed description of the heterotropic allosteric transition in which structural flexibility plays a central role. The T conformer's external zone [Horjales *et al.* (1999), *Structure*, **7**, 527–536] presents higher *B* values than in the R conformers. The ligand-free enzyme (T conformer) undergoes an allosteric transition to the free active-site R conformer upon binding of the allosteric activator. This structure shows three alternate conformations of the mobile section of the active-site lid (residues 163–182), in comparison to the high *B* values for the unique conformation of the T conformer. One of these alternate R conformations corresponds to the active-site lid found when the substrate is bound. The disorder associated with the three alternate conformations can be related to the biological regulation of the K_m of the enzyme for the reaction, which is metabolically required to maintain adequate concentrations of the activator, which holds the enzyme in its R state. Seven alternate conformations for the active-site lid and three for the C-terminus were refined for the T structure using isotropic *B* factors. Some of these conformers approach that of the R conformer in geometry. Furthermore, the direction of the atomic vibrations obtained with anisotropic *B* refinement supports the hypothesis of an oscillating rather than a tense T state. The concerted character of the allosteric transition is also analysed in view of the apparent dynamics of the conformers.

1. Introduction

Allosteric regulation involves communication between distant ligand-binding sites on biological macromolecules, which is central to many cellular regulatory mechanisms (Perutz, 1990). It encompasses two kinds of transitions: (i) homotropic, in which binding of a molecule to one subunit modulates the binding of the same type of molecule to the other subunits, and (ii) heterotropic, in which binding of a ligand in its specific site triggers a conformational change that modulates the binding properties of a second type of molecule in the binding site (Goodsell & Olson, 2000). In allosteric enzymes, this control process involves two structurally different states which differ in quaternary structure: the T form ('tense form'), in which the affinity for the substrate is zero or low, and the R form ('relaxed form') with an optimal affinity for substrate and/or allosteric activator. The metabolic regulation achieved by allosteric enzymes results from their ability to shift the

system equilibrium between these two states through the homotropic route (active-site ligand bound) or through the heterotropic route (allosteric site ligand bound). The traditional concept of allosteric transition could explain quantitatively many of the observed cooperative and linkage phenomena in allosteric enzymes, but even in the original paper Monod emphasizes that

> the concept of conformational transition should be understood in its widest connotation

(Monod *et al.*, 1965). Actually, we know that individual macromolecules are dynamic objects that undergo various forms of intramolecular motion (Jencks, 1997). In some cases, the effect of these motions can be directly correlated with enzyme activity and protein function (Ji *et al.*, 1998; Blow, 2000).

The allosteric transition concept and the concerted allosteric model of Monod *et al.* (1965) were introduced 35 y ago to explain available kinetic data in a time of very limited macromolecular structural information. This model describes the thermodynamic equilibrium between the T and R states; its application to enzymatic kinetic processes is possible under the assumption that the enzyme follows rapid equilibrium rather than steady-state kinetics (Noat *et al.*, 1968). Steady-state kinetic equations for allosteric enzymes are of great complexity and present very limited practical use, with some exceptions which use the steady-state kinetic equations in a classical approach, introducing the cooperativity components into the model in an empirical way (Willemoes *et al.*, 2000; Tovar-Mendez *et al.*, 1998). The Monod–Wyman–Changeux model, together with the contemporary sequential Koshland–Nemethy–Filmer model (Koshland *et al.*, 1966), are still used, with or without modifications, to explain the allosteric behaviour of most of the allosteric enzymes (Yifrach & Horovitz, 1995; Perella & Di Cera, 1998). We want to emphasize that both T and R states are characterized by a specific quaternary structure, but this can be achieved in different ways. For example, the R state can be obtained when the allosteric activator is bound, when active-site ligands (substrate or competitive inhibitor) bind or when both active and allosteric sites are occupied. These three complexes share the same quaternary structure, but they can present local tertiary structural differences and different mobilities of those structural components. These local differences have not been analysed in detail for many allosteric enzymes. They involve general differences in binding properties which kinetically are expressed in a ΔG (Gibbs free energy) which contains differences between the two states of the T–R transition (Bustos-Jaimes & Calcagno, 2002), with regard to both enthalpic and entropic terms. When the protein reaches the R conformer either through the heterotropic or the homotropic route, the binding of a new substrate is independent of the way in which the R conformer was obtained, resulting in the same $V_{\max}$ through homotropic or heterotropic activation. If the enzyme follows the MWC model (Monod *et al.*, 1965) this results in a K system. Conversely, if local differences in conformation or atomic mobility are found in different R complexes, the kinetic process can present differences in relation to the way in which the R conformer was obtained. This can result in V-type activation or mixed K–V systems.

The experimentally obtained *B* values (or thermal components) generated for each atom during the X-ray crystallographic refinement of a protein model, even with its limitations, are directly related to the thermal vibration of each atom in the crystal and can be associated with the entropy change of a particular process related to the molecule (Rubinson, 1998). Anisotropic calculations can provide information on the direction of molecular flexibility. A sufficient redundancy of reflection data compared with model parameters is necessary to obtain reliable values for *B* factors (Kidera & Go, 1992). Thus, a comparison between the stable conformations in which the protein crystallizes and the kinetically defined states (R and T) can provide information on conformational and vibrational changes associated with the allosteric transition. Conformational changes associated with allosteric enzyme regulation have been studied in several cases such as phosphoribosyl diphosphate synthase (Willemoes *et al.*, 2000), glycogen phosphorylase (Rath *et al.*, 2000), fructose 1,6-bisphosphatase (Choe *et al.*, 2000), phosphofructokinase (Kimmel & Reinhart, 2000), pyruvate kinase (Valentini *et al.*, 2000) and aspartate transcarbamoylase (Sakash & Kantrowitz, 2000; Endrizzi *et al.*, 2000). Unfortunately, in most of the cases the complexity of the structures and the irreversible character of the reactions catalysed disable the inclusion of atomic vibrations in the description of the allosteric transition. In this context, 2-amino-2-deoxy-D-glucose-6-phosphate aminohydrolase (ketol isomerizing) or glucosamine-6-phosphate deaminase (GlcN6P deaminase; E.C. 3.5.99.6, formerly E.C. 5.3.1.10) from *E. coli* is a well studied model from genetic, kinetic and structural points of view (Horjales *et al.*, 1999; Oliva *et al.*, 1995; Altamirano *et al.*, 1994; Montero-Morán *et al.*, 1998; Midelfort & Rose, 1977; Calcagno *et al.*, 1984; Altamirano *et al.*, 1995; Plumbridge, 1990). This enzyme catalyses the reversible isomerization–deamination of glucosamine 6-phosphate (GlcN6P) to form fructose 6-phosphate (Fru6P) and ammonium ion. The functional particle is an homohexamer (266 residues per monomer) and its allosteric activator is *N*-acetylglucosamine 6-phosphate (GlcNAc6P) (Altamirano *et al.*, 1995). This molecule binds exclusively to the R form and the enzyme behaves as a typical K-system enzyme (Calcagno *et al.*, 1984). The GlcN6P deaminase homotropic cooperativity and GlcNAc6P activation can be explained in terms of the MWC model (Calcagno *et al.*, 1984). Its activity has a central role in the coordinated regulation of amino-sugar synthesis and utilization in bacteria as the only allosteric enzyme in the catabolic route. We previously reported the structure of the R state of GlcN6P deaminase in three different complexes, with both active and allosteric sites occupied by ligands, in a range between 2.10 and 2.40 Å resolution (Oliva *et al.*, 1995) and the ligand-free T conformer at 2.30 Å resolution (Horjales *et al.*, 1999). Here, we report the crystallographic structures of another five complexes of wild-type GlcN6P deaminase from *E. coli* in both the T and R states. We present the structure of

the free active-site R form (GlcNAc6P bound to the allosteric site) at 1.73 Å resolution and the ligand-free T form at higher resolution (1.90 Å). We also refined three other structures that are used in this work to validate *B*-factor comparisons. On the basis of these structures, we describe an entropic component associated with active-site ligand binding generated by the flexible behaviour of the residues in the active-site lid (residues 158–187). The relationship between the allosteric transition and the molecular flexibility changes and its biological function is also described (to obtain a structural background and for the definition of the sections of the title enzyme, see Fig. 1).

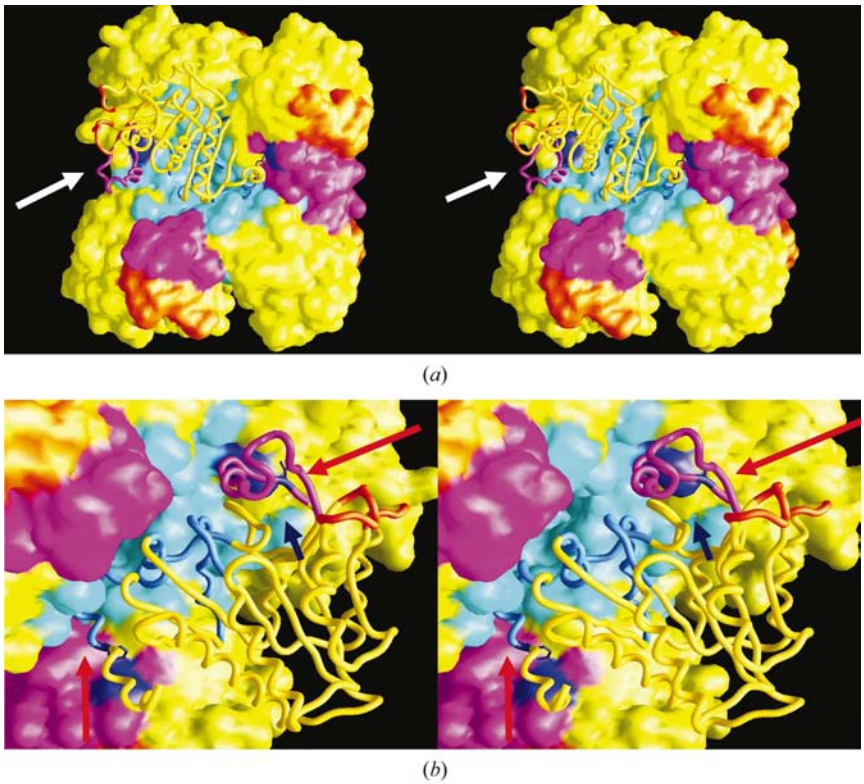

Figure 1
(*a*) Stereo drawing showing the biologically functional homo-hexameric particle of the GlcN6P deaminase from *E. coli* and (*b*) a close-up view of a monomer. The colours are as follows: cyan, the internal module, which is responsible for most of the intermonomeric contacts of the hexamer (residues 137–143, 207–233 and 244–253); magenta, the active-site lid, which has residues in the active and allosteric sites and shows an unusual flexibility behaviour during the allosteric transition (present work) [residues 158–187; the active-site lid is formed by the base of the active-site lid, which is part of an antiparallel β-sheet (residues 158–162 and 183–187), and the mobile section of the active-site lid (residues 163–182)]; orange, two loops which present large flexibilities associated with the movements of the active-site lid (present work) (residues 75–83 and 109–112); yellow, the external module, which describe a rotation of 11° during the allosteric transition (Horjales *et al.*, 1999) (residues 1–136, 144–206, 234–243 and 254–266); dark blue, the residues Tyr254 (at the beginning of the C-terminus) and Thr161 (at the active-site lid), which in the R form build an inter-monomeric hydrogen bond (Montero-Morán *et al.*, 1998) as part of a complex water-mediated hydrogen-bond net. In the T form a different intersubunit hydrogen-bond network exists which includes a hydrogen bond between residues Tyr254 and Pro149 (Montero-Morán *et al.*, 1998). In (*a*), the white arrow shows the viewpoint of figure (*b*). In (*b*), the red arrow points to the allosteric site (residues 1, 158 and 160), which is functional only in the R conformer (Oliva *et al.*, 1995), while the blue arrow points to the active site (residues 40–44, 72, 85, 143, 172 and 208; Oliva *et al.*, 1995). The allosteric site is formed in the intersubunit space; thus, each monomer is part of two allosteric sites. The figure was generated with *GRASP* (Nicholls *et al.*, 1993).

2. Material and methods

2.1. Preparation of the enzyme before crystallization trials

The two final steps in the process of purification of GlcN6P deaminase include its elution from an affinity column using its allosteric activator (GlcNAc6P) as exchanger. Finally, the enzyme is precipitated with ammonium sulfate and stored at 277 K (Calcagno *et al.*, 1984). The pure *E. coli* GlcN6P deaminase precipitated with ammonium sulfate is exhaustively dialysed at 277 K with six changes (1:1000 volume) 100 m*M* HEPES pH 7.0. The intervals between each change are 4, 12, 4, 4, 4 and 12 h. In some cases where this protocol was not followed, we obtained crystals with sulfate ions or GlcNAc6P bound. The final enzyme solution is then used for the crystallization trials.

2.2. Crystallization and structure determination

E. coli GlcN6P deaminase crystallizes in its T or R conformers as follows: wild-type R-form crystals with GlcNAc6P (2.20 Å resolution) were grown at 291 K in 2.8 *M* sodium acetate, 100 m*M* HEPES pH 7.5, with unit-cell parameters $a = b = 125.700$, $c = 224.000$ Å, $\alpha = \beta = 90$, $\gamma = 120°$. Wild-type R-form crystals with GlcNAc6P (1.73 Å resolution) were grown at 291 K in 0.75 *M* sodium tartrate, 200 m*M* HEPES pH 7.0 and 50 µ*M* GlcNAc6P, with unit-cell parameters $a = b = 124.228$, $c = 222.724$ Å, $\alpha = \beta = 90$, $\gamma = 120°$. Wild-type T-form crystals (2.20 Å resolution) were grown at 291 K in 2.45 *M* sodium acetate, 100 m*M* HEPES pH 6.8, with unit-cell parameters $a = b = 126.8$, $c = 139.44$ Å, $\alpha = \beta = 90$, $\gamma = 120°$; the crystals were soaked in 10 m*M* Fru6P and then exposed to X-rays. Wild-type R-form crystals with Fru6P were grown at 291 K in 2.8 *M* sodium acetate, 100 m*M* HEPES pH 7.5 and 27 m*M* Fru6P, with unit-cell parameters $a = b = 126.04$, $c = 223.508$ Å, $\alpha = \beta = 90$, $\gamma = 120°$. Wild-type T-form crystals (1.90 Å resolution) were grown at 291 K in 2.45 *M* sodium acetate, 100 m*M* HEPES pH 6.8, with unit-cell parameters $a = b = 126.676$, $c = 139.326$ Å, $\alpha = \beta = 90$, $\gamma = 120°$. All the native R-form crystals belong to space group *R*32 with one dimer in the asymmetric unit, while the native T-form crystals belong to space group $P6_322$ with one monomer in the asymmetric unit, in both cases generating the biologically active homohexamer by crystal symmetry. In all cases the crystals grew using the vapour-diffusion technique with 5–10 µl drops containing 15 mg ml^{-1}

Table 1
Data collection and processing.

Values in parentheses are for the highest resolution bin.

Conformer	R	R	R	T	T	
Monomers in asymmetric unit (AU)	2	2	2	1	1	
Active-site ligand	Fru6P	Empty	Empty†	Empty	Empty	
Allosteric site ligand	Fru6P	GlcNAc6P	GlcNAc6P	Empty	Empty	
Other ligands found in the AU	None	None	1 tartaric acid	None	None	
Cryocollection/X-ray source‡	Yes/SSRL 7-1	Yes/SSRL 7-1	Yes/SSRL 9-1	Yes/SSRL 7-1	Yes/SSRL 9-1	
Cryoprotectant§	Sucrose, 35%	Sucrose, 35%	Trehalose, 35%	Sucrose, 35%	Trehalose, 35%	
Space group	*R*32	*R*32	*R*32	$P6_322$	$P6_322$	
Unit-cell parameters, $a = b$, c (Å)	126.04, 223.50	125.70, 224.00	124.22, 222.72	126.8, 139.44	126.68, 139.33	
Resolution (Å)	50–2.15 (2.15–2.20)	50–2.10 (2.10–2.25)	50–1.73 (1.73–1.77)	50–2.10 (2.10–2.25)	50–1.90 (1.90–1.95)	
R_{sym}	0.071 (0.221)	0.087 (0.305)	0.083 (0.284)	0.067 (0.316)	0.072 (0.326)	
Completeness (%)	94.6 (97.2)	90.5 (72.3)	95.6 (86.3)	94.5 (70.8)	93.1 (91.2)	
Multiplicity (all data)	2.9	2.6	3.5	3.7	3.4	
$I/\sigma(I)$	8.1 (3.6)	6.77 (2.5)	8.1 (2.9)	9.64 (2.4)	6.9 (2.3)	
No. of reflections	35080	31426	65814	31742	48346	
Rigid-body minimization¶	$R = 0.279$	$R = 0.279$	$R = 0.310$	$R = 0.288$	$R = 0.322$	
Annealing ($T_i = 2000$ K)	$R = 0.226$, $R_{free} = 0.271$	$R = 0.266$, $R_{free} = 0.286$	$R = 0.298$, $R_{free} = 0.308$	$R = 0.226$, $R_{free} = 0.281$	$R = 0.275$, $R_{free} = 0.263$	
Ligand search or manual corrections	$R = 0.208$, $R_{free} = 0.260$	$R = 0.246$, $R_{free} = 0.267$	$R = 0.238$, $R_{free} = 0.271$	$R = 0.220$, $R_{free} = 0.251$	$R = 0.224$, $R_{free} = 0.244$	
Water search	$R = 0.187$, $R_{free} = 0.233$	$R = 0.199$, $R_{free} = 0.228$	$R = 0.212$, $R_{free} = 0.231$	$R = 0.214$, $R_{free} = 0.235$	$R = 0.218$, $R_{free} = 0.238$	
					Aniso. ref.††	Mult. alt. conf. ref††
Water molecules (in AU)	304	234	682	168	297	294
Reflection-to-parameter ratio	1.95	1.77	3.22	3.55	5.02	5.02
Multiple alternate conformation construction in the active-site lid	—	—	$R = 0.195$, $R_{free} = 0.227$	—	—	$R = 0.211$, $R_{free} = 0.229$
Anisotropic refinement	—	—	—	—	$R = 0.188$, $R_{free} = 0.233$	—
Multiple alternate conformation construction in the active-site lid and C-terminus	—	—	—	—	—	$R = 0.209$, $R_{free} = 0.225$
Reflection-to-parameter ratio after multiple conformation or anisotropic refinement	—	—	2.50	—	2.23	2.57
PDB code	1fqo	1frz	1fs5	1fs6	1fsf	—

† In one monomer of the asymmetric unit the active site is occupied by one molecule of tartaric acid and the other monomer presents a ligand-free active site. ‡ All the diffraction data were collected at 103–113 K. The test data set for R_{free} calculations was randomly selected to contain 10% of the whole data set. § In all cases the cryoprotectant solution is the same as the mother liquor where the crystals grew, but instead of water the salts were dissolved in aqueous solutions of sucrose or trehalose. ¶ The rigid-body minimizations were performed directly using as starting models the R and T structures previously reported by our group (PDB codes 1hot and 1cd5). In each step of the refinement procedure, manual adjustments were performed using both $2F_o - F_c$ and $F_o - F_c$ electron-density maps. †† Statistics for two different refinement procedures of the same data-set: Aniso. ref., using the anisotropic model for *B*-factor refinement; Mult. alt. conf. ref., using the isotropic model with alternate conformations of the active-site lid and the C-terminus.

protein. In all cases the crystal morphology, size and growth time were identical to previously reported GlcN6P deaminase R-form (Oliva *et al.*, 1995) and T-form (Horjales *et al.*, 1999) crystals.

Diffraction data were obtained at the Stanford Synchrotron Radiation Laboratory Station 7-1 (except data from wild-type T-form crystals at 1.90 Å resolution and wild-type R-form crystals with GlcNAc6P at 1.73 Å resolution, which were collected at Station 9-1) at liquid-nitrogen temperatures (103–113 K). In all cases the cryoprotectant solutions contained the same salts at the same concentrations as the reservoir solution but dissolved in 35% sucrose (wild-type T-form crystals at 2.20 Å resolution and wild-type R-form crystals with GlcNAc6P at 2.20 Å resolution) or 35% trehalose (wild-type T-form crystals at 1.90 Å resolution and wild-type R-form crystals with GlcNAc6P at 1.73 Å resolution). Diffraction data were collected using an image-plate detector (MAR Research, Hamburg) and the highest resolution limit for each particular data set ranged between 1.73 and 2.20 Å resolution. Table 1 shows the measurement statistics. Data were integrated using the program *DENZO* (Otwinowski, 1993; Otwinowski & Minor, 1996) and scaled with the programs *SCALA* and *TRUNCATE* from the *CCP*4 suite (Collaborative Computational Project, Number 4, 1994). The structures were solved using the previous reported structures of the GlcN6P deaminase T and R conformers (Horjales *et al.*, 1999; Oliva *et al.*, 1995) as initial models, without rotation and translation searches (owing to the similarities in the unit-cell values), by a rigid minimization procedure as shown in Table 1.

2.3. Construction of alternate conformations in the active-site lid of the heterotropic R form

The R-form structure with an empty active site and a GlcNAc6P molecule bound to its allosteric site was determined at 1.73 Å resolution and refined using the *CNS* program (Brunger *et al.*, 1998). A molecule of tartaric acid was found in the active site of the first monomer in the asymmetric unit,

while the second monomer has an empty active site (see Table 1). The active-site lid of the first monomer in the asymmetric unit presents a flexibility which is lower than the second monomer in all R structures determined. This is produced by crystallographic contacts stabilized through hydrogen bonds with a neighbouring active-site lid. This reduced flexibility favours the differential binding of the tartaric acid molecule in this monomer.

Two independent determinations of this structure [PDB codes 1fs5 (1.73 Å resolution) and 1frz (2.20 Å resolution)] presented different conformations in the region of the mobile section of the active-site lid (residues 163–182) and the neighbouring loops (residues 75–83 and 109–112), all with large B factors. An $F_o - F_c$ map (of the structure at 1.73 Å resolution) at this stage presented negative density for the refined active-site lid conformation and positive density close to the conformation corresponding to the structure determined at 2.20 Å resolution. Thus, the mobile section of the active-site lid has at least two alternate conformations. Including these two conformations in the refinement of the structure at 1.73 Å resolution, a third alternate conformation clearly appears in the $F_o - F_c$ map (see Fig. 5). This search was also performed with the R form with both sites occupied by phosphate ions at 1.65 Å resolution (Rudiño-Piñera & Horjales, unpublished work), but only one active-site lid conformation was found without remarkable density around the lid in the $F_o - F_c$ map.

2.4. Anisotropic refinement

The final model from the wild type T-form crystals at 1.90 Å resolution obtained with *CNS* (R = 0.218, $R_{\rm free,\,10\%}$ = 0.238 with data higher than 2σ) was used to carry out a new refinement (with the same reflection file and $R_{\rm free}$ test group from *CNS*) using the program *SHELXL*97 (Sheldrick & Schneider, 1997). An initial isotropic minimization was performed, followed by a set of cycles refining anisotropically only the S atoms, with *CNS* minimizing cycles to avoid over-refinement. Finally, using the same water-molecule set (297 water molecules) generated by *CNS*, all non-H atoms were refined anisotropically. This last refinement was performed in short cycles to reduce the problems that could be caused by the parameter-to-reflection ratio. The final R and $R_{\rm free,\,10\%}$ values were 0.188 and 0.233, respectively, with data higher than 2σ. Starting from the structure with 297 water molecules, we applied a two different anisotropic refinements, one including only the mobile section of the active-site lid (residues 163–182) and the other only the C-terminus (residues 245–266). The results of these refinements show the same direction and B values as in the anisotropic refinement of the whole monomer (data not shown).

2.5. Refinement of alternate conformations for the active-site lid and the C-terminus

Starting from the refined T-form structure at 1.90 Å resolution including temperature factors (see Table 1), we constructed three alternate conformations for residues 159–186 in two different ways: (i) the refined conformer plus two alternate conformations displaced 0.80 Å in the direction of the larger anisotropic ellipsoid axis at both sides of the original one and (ii) as (i) but displaced in a perpendicular direction. Trial (i) reduced both R and $R_{\rm free}$ values, while trial (ii) increased both. We added as many alternate conformations as necessary to obtain no interpretable density peaks in an $F_o - F_c$ map contoured at 3σ. For each new alternate conformation minimize, b-individual, q-group, annealing (500 K), b-individual, q-group and finally, b-individual refinement steps were performed, resulting in seven alternate conformations. The five alternate conformations model showed a total occupancy in the lid of 0.86 and for the seven alternate conformations model this value was 0.96. The same procedure was followed for the C-terminus, obtaining three alternate conformations for residues 254–266. In each of the mentioned steps both the R and $R_{\rm free}$ values decreased slightly (see Table 1). It is remarkable that q-values for each alternate conformations were quite independent of the number of conformers included in the model.

3. Results

3.1. Determination and analysis of the structures

All the R-state crystals of the GlcN6P deaminase from *E. coli* belong to the *R*32 space group with a dimer in the asymmetric unit. In contrast, T-form crystals belong to the $P6_322$ space group with only one monomer in the asymmetric unit (Horjales *et al.*, 1999). In the case of the R forms, the root-mean-square deviation (RMSD) of the C^{α}-atom superposition between both monomers of the asymmetric unit results in a value of 0.305 Å (266 C^{α} atoms in the calculation) for the structure with both active and allosteric sites occupied (present work at 2.15 Å resolution) and 0.494 Å (266 C^{α} atoms in the calculation) for the structure with only the allosteric site occupied (present work at 2.20 Å resolution). These structural differences are probably related to the occupancy of the active site or to the crystal packing. Some reports suggest criteria that allow the discrimination of conformational changes arising from ligand binding from those associated with the crystal packing in each monomer (Eigenbrot *et al.*, 1992). In order to analyse the origin of these differences, we compared both monomers in the R-form asymmetric unit of one structure with its corresponding monomer in the second structure (PDB codes 1fqo and 1frz). Some main-chain differences larger than 0.70 Å in the first monomer of the R asymmetric unit can be assigned to crystal contacts. In contrast, in the second monomer we observed just a few crystallographic contacts that did not present main-chain conformation modifications greater than 0.10 Å. In the first monomer, some of these contacts with other hexameric particles include residues from the mobile section of the active-site lid (residues 163–182) and are mediated by ordered water molecules. Otherwise, the second monomer presents neither distortion nor crystal contacts mediated by the active-site lid. Additionally, the behaviour of the B-factor values for both GlcN6P deaminase

R forms clearly presents differences between the two independent monomers of the asymmetric unit (Fig. 2*a*). When the active-site lid is free of crystal contacts, as in the second monomer of the R form, its *B* values rise. Thus, in the subsequent sections, we will compare the conformations and the atomic vibrations of the monomer in the T state with the second monomer in the asymmetric unit of R conformers.

3.2. Attempts to obtain T-state crystals with occupied active site

As the parameter *c* in the adjustment of the MWC model is not zero ($c = 0.02$), the existence of molecules in the T state, with ligand bound to the active site, adjusts the kinetic data in a better way (Montero-Morán *et al.*, 1998). From a crystallographic point of view, we attempted to detect this occupied active-site T state. The search for crystallization conditions which contain the ligands of the active site in the mother liquor, such as Fru6P or 2-deoxy-2amino-D-glucitol-6-phosphate (GlcNol6P), always resulted in R-state crystals, even at low concentrations. At very low concentrations only ligand-free T crystals were obtained (data not shown). Thus, we changed the strategy: we soaked a T crystal in solutions with 10 m*M* Fru6P and 100 µ*M* GlcNol6P. In both cases the crystals did not lose their diffraction properties. In the case of the T-state crystals soaked with GlcNol6P, diffraction data were collected and refinement resulted in a T protein model at 2.80 Å resolution (data measured using a rotating-anode generator) with a final $R = 0.211$ ($R_{\rm free} = 0.240$). This structure did not have any GlcNol6P molecule in the active or allosteric sites (even at this low resolution, the phosphate groups should be detected). For the T form soaked in 10 m*M* Fru6P, the final protein model at 2.20 Å resolution also resulted in a ligand-free T structure.

3.3. Behaviour of isotropic *B* values: vibrational changes associated with substrate binding

In order to perform a conformational and vibrational comparison between T and R conformers, we used structures (PDB codes 1fqo, 1frz and 1fs6) which were determined under the same conditions of X-ray data collection, crystal cryoprotectant and similar resolution limits. A C^{α} superimposition shows that the differences detected between the main-chain positions in the models correspond to residues where the *B* factors are higher than 35 Å^2 (Figs. 2*b* and 3). In particular, the *B*-factor values in the active-site lid decrease upon active-site ligand binding. The *B*-factor distribution in the ligand-free T structure presents a highly vibrating active-site lid (residues 158–187). When this vibration is compared with a purely heterotropic R-form structure (free active site), the *B* factors of the active-site lid are still high. In the case of an R form with both sites occupied, the *B*-factor values decrease from close to 75 Å^2 in the purely heterotropic R form to close to 45 Å^2. It is also important to emphasize that the binding at both sites clearly produces a reduction of the general isotropic *B* factors throughout the structure (see Fig. 2*b*). In this particular case the baseline of the *B* factors is at 10 Å^2, while in the other structures with the active or the allosteric site empty this baseline is close to 18 Å^2. This effect is also found in the three structures which originally describe the R form of the GlcN6P deaminase from *E. coli*, which were collected at 27 K (Oliva *et al.*, 1995). Thus, the ligand-free T conformer is the structure with highest molecular flexibility.

We tried to grow crystals of the homotropic R form (free allosteric site), as this structure would provide information on the dependence of the vibrational change at the active-site lid with allosteric activator binding. Extensive trials to obtain wild-type protein crystals in this form have not been successful. The mutant Lys160Glu (Lara-González *et al.*, unpublished work) changes the electrostatic surface, affecting a residue with a central role in binding the activator (GlcNAc6P) to the allosteric site. Its final structure in the R form with only the active site occupied, collected and solved at identical conditions as the other structures in this section, presents *B*-factor behaviour almost identical to that of the wild-type R form with both sites (active and allosteric sites) occupied (see Figs. 2*b* and 3), but with a baseline almost at 18 Å^2. This means that the flexibility of the active-site lid can be highly reduced just through binding of a ligand in the active site. A similar feature is observed in fructose 1,6-bisphosphatase: a structural section (in this case a loop) which is highly mobile in the T form and fixed in the R form. This change is also related to substrate binding (Choe *et al.*, 2000).

In previous work, we presented the allosteric transition as a rotation of the external region of each monomer around an axis perpendicular to the crystallographic *c* axis (Horjales *et al.*, 1999). As described above, the T-form structure only presents a higher mobility in the external section and the active-site lid, which may be related to some properties of the allosteric transition. With this in mind, we tried to find a probable centre of rotation of the observed T-form flexibility. We used the atom with the lowest *B* value (C^{α} residue 226, which is in the internal section of the enzyme) as placed at the rotation axis (parallel to the crystallographic *c* axis). We calculated the distances between this rotation axis and the rest of the C^{α} atoms. Fig. 4 shows a plot of the corresponding isotropic *B* values of the main chain as a function of these distances (we used main-chain atoms to avoid noise generated by side-chain local vibrations). The final plot describes a linear distribution in which *B* isotropic values increase with distance to an axis parallel to the crystallographic *c* axis. It can be interpreted as a rotation which has the same centre and axis as that previously reported for the allosteric transition (Horjales *et al.*, 1999).

3.4. Heterotropic free active-site R form: multiple alternate conformations at the active-site lid

In the R form with both sites occupied, residue Glu148 is an essential structural element in the stabilization of the active-site lid. It points to the active-site pocket, forming hydrogen bonds between the $O^{\delta1}$ and N atoms of residues Thr166 and Thr163 at the lid and the $N^{\delta1}$ atom of the active-site residue His143, contributing to the stabilization of the full lid. In this

position, Glu148 has been proposed to form an uncommon proton relay which is directly related to enzymatic catalysis (Oliva *et al.*, 1995). In the T form, Glu148 points to the allosteric site, equilibrating the charges in the pocket (Horjales *et al.*, 1999) and disrupting the bridge between His143 and the base of the active-site lid. This conformational change of the main chain of Glu148 contributes to the high flexibility found in the active-site lid T conformation. In the R form with only the allosteric site occupied, the position of the residue Glu148 is the same as in the R form with both sites occupied, but only one of the active-site lid alternate conformations forms hydrogen bonds with Thr166 and Thr163. This means that the absence of an active-site binding molecule

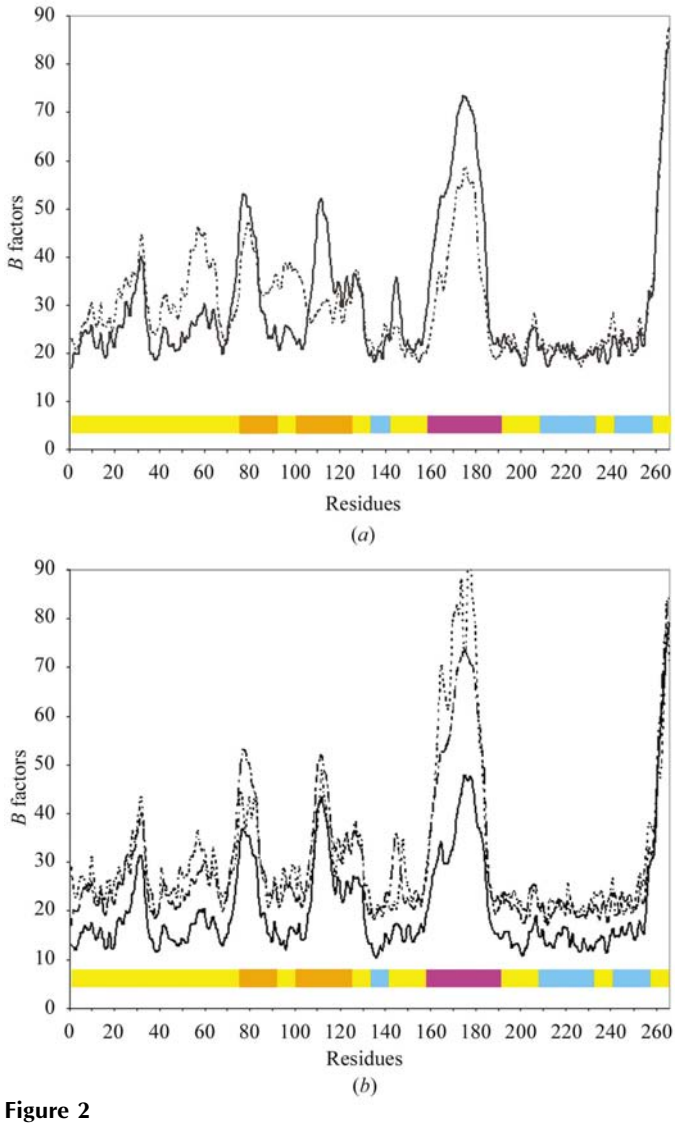

Figure 2
(*a*) The *B*-factor distributions along the sequence of the R state of *E. coli* GlcN6P deaminase, with the allosteric site occupied. The first monomer of the asymmetric unit (dashed line) and the second (full line) are presented (PDB code 1frz). (*b*) The *B*-factor distributions along the sequence of the R state *E. coli* GlcN6P deaminase with both sites occupied (full line; PDB code 1fqo), the R state with the allosteric site occupied (dashed–dotted line; PDB code 1frz) and the T form (dashed line; PDB code 1fs6); we used the second monomer of the asymmetric unit for the R forms. All the structures used have similar resolutions and their diffraction patterns were collected at identical conditions on the same SSRL 7-1 beamline under liquid-nitrogen conditions. Colour code: yellow, the external section; cyan, the internal section; magenta, the active-site lid and orange, the active-site lid neighbouring loops. See Table 2 and Fig. 1.

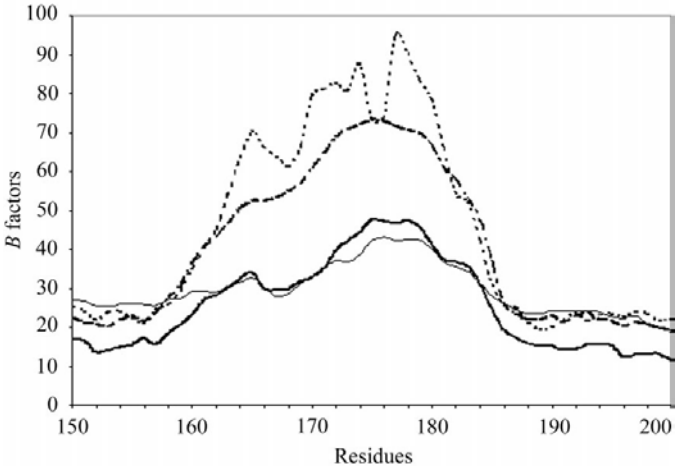

Figure 3
Average *B* factors for main-chain atoms are presented for the wild-type T form at 2.20 Å resolution (thick dashed line), the wild-type R form with only the allosteric site occupied at 2.20 Å resolution (thin dashed line), the wild-type R form with both active and allosteric sites occupied at 2.15 Å resolution (thick full line) and the mutant Tyr160Glu (Lara-Gonzalez *et al.*, unpublished work) with only the active site occupied at 2.30 Å resolution (thin full line). All data sets were collected at SSRL beamline 7-1 at liquid-nitrogen temperatures using 35% sucrose as cryoprotectant solution; the structures were solved with *CNS*. Isotropic temperature *B* factors are plotted for the active-site lid (residues 158–187).

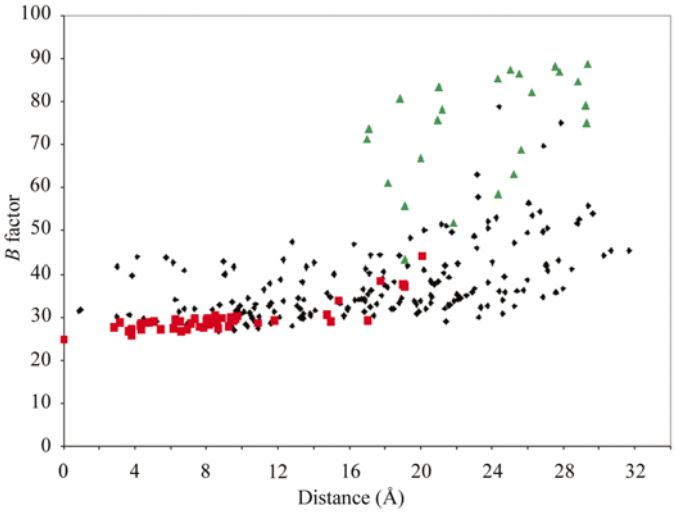

Figure 4
The plot represents the *B*-factor values as a function of the distance of each C^{α} atom from an axis parallel to the crystallographic *c* axis going through the atom with lowest atomic mobility. The internal section (red squares) and the external section (black rhombi) of the T state of the enzyme (present work at 1.90 Å resolution) describe an increase of the vibration in relation to the distance to the less mobile residue. The active-site lid (green triangles) presents a stronger vibrational motion in the same plane. When the plotted data of the external section (without the C-terminus and active-site lid) is adjusted to a linear distribution, the resulted slope is 0.4674 (correlation factor = 0.2596). In all the R cases (data not shown) the slope always is less than 0.0800.

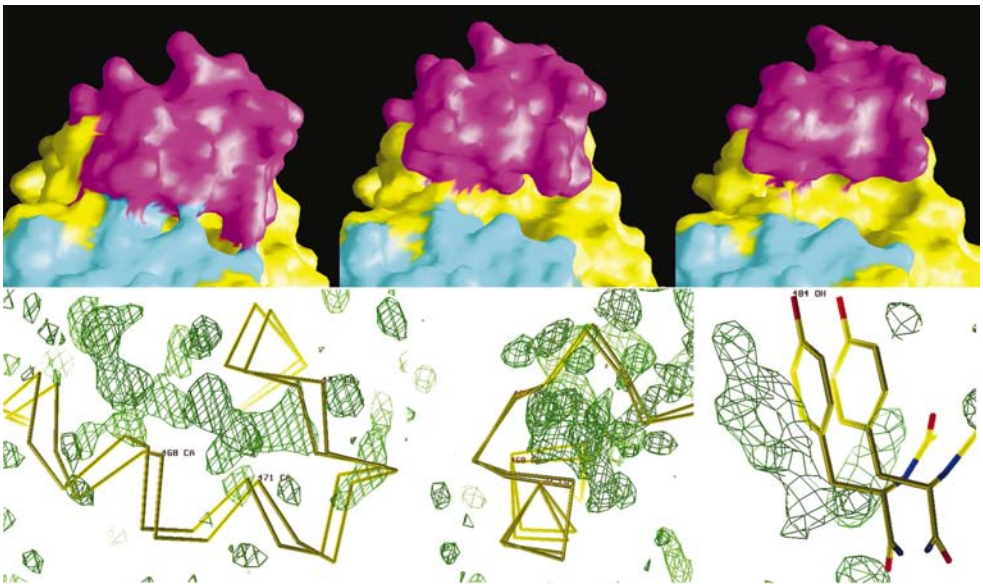

Figure 5
The alternate active-site lids found in the R-form enzyme, with only the allosteric site occupied at 1.73 Å resolution. The solvent-access surface figure (top) presents the three conformers describing an opening/closing movement in the active-site lid. The second set of figures (bottom) presents the construction of the third alternate active-site lid. Here, an $F_o - F_c$ map shows a sufficiently positive electron density to construct another conformation; even the lateral chain presents a clear third alternate structure. Colour code as in Fig. 1.

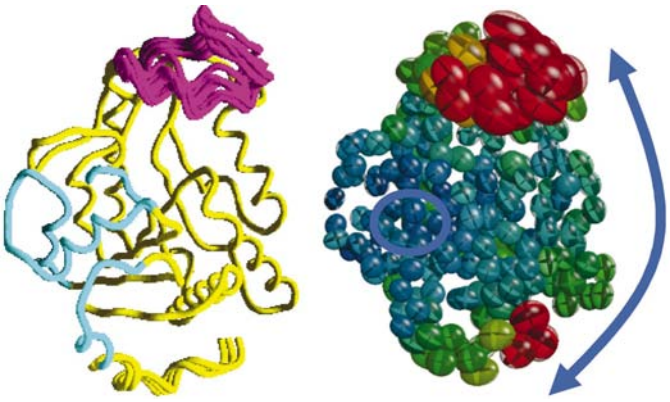

Figure 6
Left: view of the trace of the ligand-free T-form monomer of GlcN6P deaminase, refined with alternate conformations at both the active-site lid and the C-terminus. Colour code: yellow, external section; cyan, internal section; magenta, active-site lid. See Fig. 1. Right: after an anisotropic refinement, the C^{α} atoms of the ligand-free T form clearly show a rotation movement with the axis at the centre of the small blue circle which is similar to that proposed for the allosteric transition (Horjales *et al.*, 1999). The trace is coloured according to isotropic *B*-factor values: red for high and blue for low values. C^{α} *B*-factor values range from 24 to 148 Å^2.

prevents complete stabilization of the active-site lid. Thus, in the T to R allosteric transition the active-site lid moves from a highly mobile state (T form), to a less mobile state partially stabilized by the bridge mediated by Glu148 (purely heterotropic R form) and finally to an active-site lid fully stabilized by both ligands and bridge at Glu148.

3.5. Further refinement of the T form: anisotropic *B* refinement and multiple alternate conformations

We performed an anisotropic refinement of the non-H atoms in order to generate additional data to clarify whether the atomic vibration of the active-site lid can be correlated to the allosteric transition, using data from the T form at 1.90 Å resolution. This crystal has 78% water content, which means that the 2411 atoms generate the whole structure in a large unit cell (for this number of atoms). Thus, at 1.90 Å resolution we collected 48 412 reflections, an average of 20 reflections for each atom. At this resolution, H atoms are not detectable. Moreover, there are isotropic *B* factors over 80 Å^2 in large regions of the structure (active-site lid and C-terminus). Atoms with such high isotropic mobility should produce different diffraction patterns at such resolution to those with high anisotropic mobilities. The high solvent content in the crystal favours the mathematical possibility of refining the anisotropic *B* factors: for each atom we need to calculate nine parameters (x, y, z and the six anisotropic terms), therefore overall we have to calculate 21 699 parameters, *i.e.* there are 2.23 reflections for each parameter. Even with this ratio of parameters to be calculated to number of reflections at 1.90 Å resolution, we can find a unique solution for the refinement procedure. For those u values of the order of 2 Å, even at 1.90 Å resolution the anisotropic description will generate a better representation of the protein model than the corresponding isotropic *B* values.

The final model refined with anisotropic *B* factors shows large values compatible with a collective rotation movement parallel to the crystallographic c axis, which includes the active-site lid, the whole external section (Oliva *et al.*, 1995) and the C-terminus of the enzyme (see Fig. 6). These regions of the monomer contain the whole allosteric site, which is placed in the intersubunit interface. In particular Tyr254 and Thr152 are involved in specific inter-monomeric interactions. Thus, this collective movement can be propagated through the whole hexamer. It is remarkable that this anisotropic movement is coincident in direction with that exerted by the same section of the monomer during the allosteric transition. The centre of this movement is coincident with that determined above using isotropic *B* factors (see §3.3) and also with that previously determined for the rotation generating the allosteric transition (Horjales *et al.*, 1999). Moreover, mutants which present lower isotropic *B* values in the active-site lid

also show lower isotropic B values in the external section, which suggests that the highly mobile active-site lid in the T form is part of a collective motion which also comprises the external section (data not shown), as in the allosteric transition. It is remarkable that even in the crystal, the anisotropic atomic vibration of the ligand-free T form describes a motion in the direction of the allosteric transition.

We also refined seven alternate conformations for the active-site lid and three alternate conformations for the C-terminus in an isotropic model (see §2 and Fig. 6). In particular, those alternate conformations found in the active-site lid present distances between 1.60 Å in the base of the lid and 4.00 Å in the residue 172, all in the same plane of the maximal anisotropic axis. In spite of the short distance between neighbouring conformers (less than 1 Å), the isotropic B factors do not fall below 55 Å^2. This can be interpreted as a continuous density rather than a set of individual conformers. This fact supports the results found in the anisotropic refinement, at least for these two regions.

3.6. MWC concerted allosteric model and GlcN6P deaminase from *E. coli*

The structural modifications which produce the transition between the ligand-free T conformer and the R conformer with both sites occupied have been described (Horjales *et al.*, 1999; Oliva *et al.*, 1995), but the concerted character of the allosteric transition lacks a structural explanation. During the rigid-body rotation associated with the T–R conformational changes, the internal section contacts do not change, but large changes are produced in the inter-monomeric contacts of the external section of the enzyme, which are directly related to the formation of the allosteric cleft (see Table 2; Horjales *et al.*, 1999). As shown above (see §3.4), Glu148 is involved in the stabilization of the active-site lid in the R conformer and in the connection between the lid and the catalytic residue His143. In the T form, Glu148, which is part of the loop 144–154, is part of a salt bridge with Lys160 which is essential in the stabilization of this conformer (Oliva *et al.*, 1995). Loop 144–154 is formed by four turns which are conserved during the transition but change their relative positions. While turn 139–142 remains as part of the internal section, turn 144–147 moves rigidly with the external section and the active-site lid, mainly because of hydrophobic interactions around Phe146. When a C^{α} superimposition between R forms with both sites and with only the allosteric site occupied is performed, we found a correlation between the movement of residues 144–146 and the active-site lid. If the R-form active site is occupied by the substrate, turn 144–146 moves in the direction of the internal section, 'closing' the active-site lid. Correspondingly, the R form without ligands in the active-site moves its turn 144–146 in the direction of the active-site lid, 'opening' the lid. The same correlation of movements also occurs in the T form, but with larger displacements of the C^{α} position. Furthermore, this 'opening' movement of the active-site lid is directly related to an increase in its atomic mobility (see Fig. 3). It is noteworthy that the residues involved in such interactions are 100% conserved in at least 14 GlcN6P deaminase sequences known to date, ranging from bacteria to mammals (Arreola *et al.*, unpublished work).

Table 2
Distances of the hydrogen bonds formed in the inter-monomer surface close to the allosteric site in both R and T conformers of the GlcN6P deaminase from *E. coli* and one hydrophobic interaction between residues Ala150 and Phe255.

When the contacts between residues are mediated by ordered water molecules, the number of water molecules involved and the distances corresponding to each hydrogen bond are presented.

Monomer *A*	T-form interaction (distance in Å)	R-form interaction (distance in Å)	Monomer *B*
Glu148 $O^{\varepsilon 1}$	3.03	None	Tyr254 OH
Pro149 O	3.23	None	Tyr254 OH
Pro149 O	2 waters (2.59, 2.30)	None	Tyr254 OH
Pro149 O	None	4 waters, (2.94, 2.84, 2.61, 2.54, 2.72)	Lys250 O
Pro149 O	None	3 waters (2.94, 2.84, 2.69, 2.94)	Thr251 $O^{\gamma 1}$
Ala150 C^{β}	4.06	3.72	Phe255 C^{ξ}
Ala150 O	3.31	3.50	Met1 O
Ala150 O	2.76	3.02	Met N
Ser152 O^{γ}	None	2.66	His232 O
Ser152 O^{γ}	2.65	None	Pro233 O
Leu153 N	1 water (2.82, 2.76)	3.02	Gln230 O
Leu153 N	1 water (2.82, 2.76)	None	His232 O
Thr161 O	None	3.14	Tyr254 OH
Thr161 N	None	1 water (3.08, 3.11)	Tyr254 OH
Lys160 N^{ξ}	None	1 water (2.69, 3.11)	Tyr254 OH
Thr161 $O^{\gamma 1}$	None	3 waters (2.96, 2.60, 2.81, 3.11)	Tyr254 OH
Lys160 O	None	4 waters (2.96, 2.55, 2.60, 2.81, 3.11)	Tyr254 OH
Lys160 N	None	4 waters (3.19, 2.55, 2.60, 2.81, 3.11)	Tyr254 OH

In the homotropic transformation, the substrate binds to the active site, closing and reducing the atomic vibration of the active-site lid and generating a change in the conformation of the loop 144–154. This conformational change breaks the hydrogen bond between Pro149 O and Tyr254 OH, which is characteristic of the T form. Moreover, the closure of the lid changes and stabilizes the position of Lys160 and Thr161, favouring the formation of the highly stable hydrogen-bond network with Tyr254 (mediated in some sections by four water molecules; see Table 2), which has been proposed to form a switch in the allosteric transition (Montero-Morán *et al.*, 1998). Furthermore, in the T form the same residue Tyr254 forms a hydrogen bond (see Table 2) with Glu148, which is also destroyed during the conformational change of the loop 144–154, further stabilizing the formation of a new hydrogen-bond network characteristic of the R state. Molecular switches have been found in other allosteric enzymes such as the *E. coli* aspartate transcarbamoylase.

In the heterotropic transition the GlcNAc6P (allosteric activator) molecule binds to its site, displacing Glu148 from the active-site cleft, breaking its interaction with Tyr254 and starting the allosteric transition in the same fashion as in the homotropic transition. This assumption is supported by the

fact that loop 144–154 changes its main-chain position owing to a strong electrostatic repulsion, as happens between Glu148 and the phosphate ion of the allosteric activator. We proposed that in both the homotropic and heterotropic allosteric transitions, the allosteric transition transmission route implies a local induced fit of the loop 144–154 which is directly related to the behaviour of the active-site lid and the propagation of the movement of the whole hexamer particle mediated by the intersubunit contacts of the external section as described.

4. Discussion

E. coli glucosamine 6-phosphate deaminase has a remarkable role as the only allosteric enzyme in the amino-sugar catabolic route. As such, it constitutes a useful tool as a kinetic and structural model for the study of enzymatic allosteric control. Here, we describe the structures of five complexes of the enzyme in R and T states and analyse their kinetic and allosteric implications. We focus this work on the role of atomic vibrations, both in the R and T conformers.

When the enzyme is in a 'ligand-free R form', the equilibrium with the 'ligand-free T form' can be displaced in two ways: homotropically by the addition of any substrate (GlcN6P or Fru6P) or heterotropically by the addition of the allosteric activator (GlcNAc6P). We found that in the second mode the R conformer has an active-site lid with three preferential conformers, which in normal conditions open and close the active-site pocket. Upon binding to the active site, the substrate stabilizes the active-site lid in one of the three conformers, producing a general reduction in the atomic vibration of the whole protein. Thus, the active-site lid flexibility not only has a central role in the allosteric transition, but also in the substrate-binding process. Thus, the high mobility of the active-site lid and the existence of three conformers in the 'free active-site R form' results in an entropic term which is associated with substrate binding and contributes to an increase in K_m. This results in a relatively high concentration of the substrate coexisting with the activated enzyme. Thus, relatively high concentrations of GlcNAc6P (the allosteric activator) are maintained in the steady state involving deaminase and the enzyme GlcNAc6P deacetylase. In this way, catabolism of GlcNAc can take place while maintaining relatively high levels of GlcNAc6P (an intermediate in the pathway). This concentration

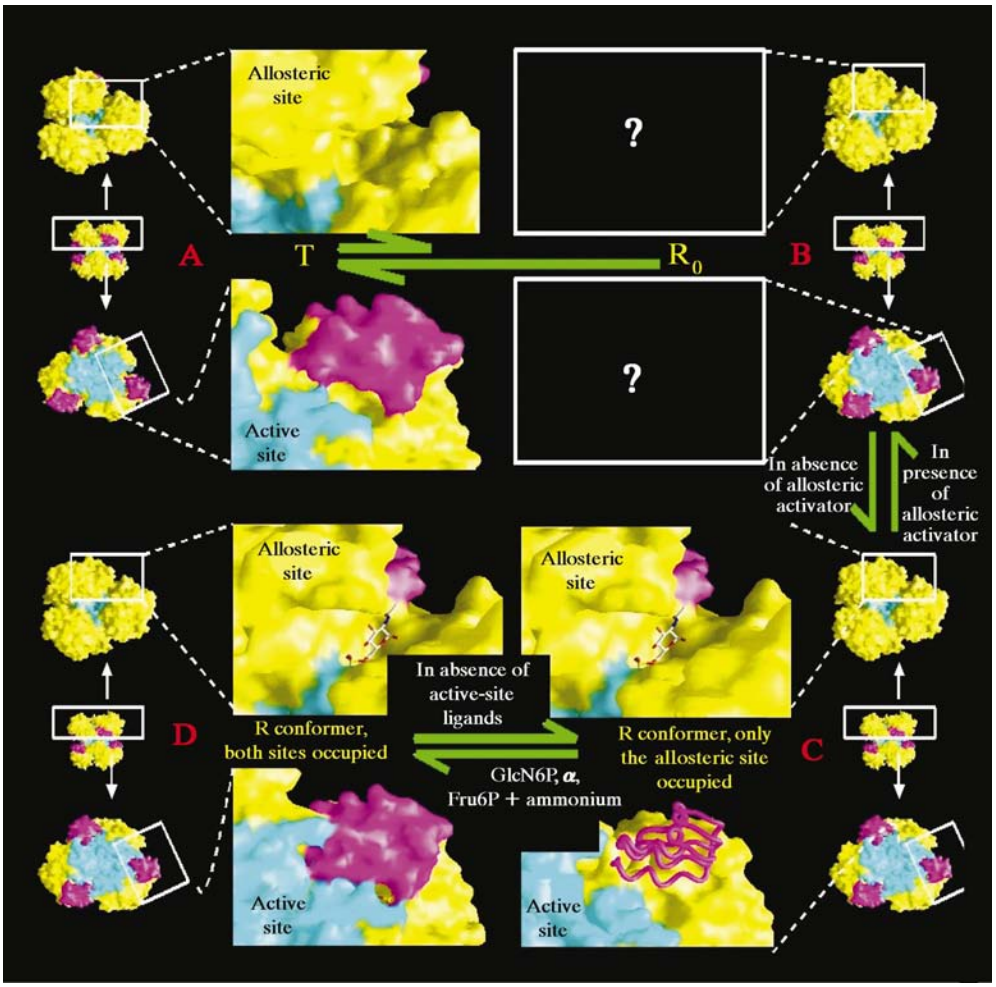

Figure 7
A, the ligand-free T form; B, the proposed ligand-free R form (A and B conformations in different concentrations form the kinetic T state); C, the R form with only the allosteric site occupied; D, the R form with both allosteric and active sites occupied (together, C and D form the R state). Assuming an MCW model, the T form is unable to bind the allosteric activator but is able to bind the substrate. In our results, we cannot obtain any T conformer with ligands bound. We propose that in both homotropic or heterotropic transformations the ligand-binding process occurs directly in a ligand-free R-form molecule, which is in equilibrium with the ligand-free T form through atomic vibrations which are in the same direction as the allosteric transformation. In the heterotropic activation the allosteric activator produces the transition from T to R; once in R, the active-site lid generates three alternate conformations 'opening' and 'closing' the active-site crevice. When the substrate (or any other ligand) binds to the active site, the lid has only one conformation, 'closing' the site (C to D). When the concentrations of substrate decrease, the empty active site generates the three alternate conformations in the lid (D to C). Finally, when the concentration of the allosteric activator further decreases, the ligand-free T form is reconstructed (C to A). Colour code: yellow, external section; cyan, internal section; magenta, active-site lid. See Fig. 1.

has to be high enough to hold the GlcN6P deaminase in its R state.

The MWC model predicts that, in solution, ligand-free T conformers of *E. coli* GlcN6P deaminase coexist in equilibrium with limited amounts of ligand-free R conformers. This kinetic model assumes that in the presence of molecules that bind to the active site, such as GlcN6P or Fru6P (homotropic transition), the 'ligand-free T form' changes to an 'occupied active-site T form', which in turn changes *via* the homotropic allosteric transition to an 'occupied active-site R form'. The crystallographic data shown here suggests that the difficulties in obtaining 'occupied active-site T form' crystals (see §2) are a consequence of one of two possible effects: either the 'occupied active-site T form' is just an unstable transition intermediate undetectable by X-ray crystallography, or the ligand-free enzyme in solution is an ensemble of structures with most of the hexameric particles in the T conformation and some in the R conformation. Thus, the homotropic allosteric transition proceeds in the sequence: 'ligand-free T form' to 'ligand-free R form' to 'occupied R form'. This is also the obligatory route for the heterotropic transition, as the allosteric activator binds exclusively to the R state (Oliva *et al.*, 1995). Thus, the presence of active-site ligands in the homotropic transition displaces the T–R equilibrium directly by binding to the active site in the 'ligand-free R conformer'. If we relate this model to the observed behaviour of the atomic flexibility found in the crystallographic ligand-free T form, it appears that the 'tense' form of the enzyme is in fact an 'oscillating' state. In this state, a minor part of the conformations involved in the oscillation reaches the 'ligand-free R form', which is the conformer that binds ligands in any of the two sites (see Fig. 7).

This research was supported by grants from PAPIIT-UNAM (IN230598), ERP and SMA are awarded with CONACyT fellowships and student research grands from PAEP (DGEP, UNAM). We wish to thank Dr M. L. Calcagno, Dr G. L. Gilliland, Dr X. Ji and Dr R. Stock for helpful discussions, Laura I. Alvarez-Añorve for supplying the purified wild-type protein and for assistance in enzyme purification, Samuel Lara-González for supplying the mutant K160E enzyme, Rodrigo Arreola for discussions, Dr M. Newcomer and the Department of Biochemistry, Vanderbilt University, Nashville, Tennessee for kind help at the initial stages of cryoprotection tests. This work is based upon research conducted at the Stanford Synchrotron Radiation Laboratory (SSRL), which is funded by the Department of Energy (BES, BER) and the National Institutes of Health (NCRR, NIGMS).

References

Altamirano, M. M., Hernández-Arana, A., Tello-Solís, S. & Calcagno, M. L. (1994). *Eur. J. Biochem.* **220**, 409–413.
Altamirano, M. M., Plumbridge, J. A., Horjales, E. & Calcagno, M. L. (1995). *Biochemistry*, **34**, 6074–6082.
Blow, D. (2000). *Structure*, **8**, R77–R81.
Brunger, A. T., Adams, P. D., Clore, G. M., Delano, W. L., Gros, P., Grosse-Kunstleve, R. W., Jiang, J. S., Kuszewski, J., Nilges, N., Pannu, N. S., Read, R. J., Rice, L. M., Simonson, T. & Warren, G. L. (1998). *Acta Cryst.* D**54**, 905–921.
Bustos-Jaimes, I. & Calcagno, M. L. (2002). In the press.
Calcagno, M. L., Campos, P. J., Mulliert, G. & Suástegui, J. (1984). *Biochim. Biophys. Acta*, **787**, 165–173.
Choe, J. Y., Fromm, H. J. & Honzatko, R. B. (2000). *Biochemistry*, **29**, 8565–8564.
Collaborative Computational Project, Number 4 (1994). *Acta Cryst.* D**50**, 760–763.
Eigenbrot, C., Randal, M. & Kossiakoff, A. A. (1992). *Proteins*, **14**, 75–87.
Endrizzi, J. A., Beernink, P. T., Alber, T. & Schachman, H. K. (2000). *Proc. Natl Acad. Sci. USA*, **97**, 5077–5082.
Goodsell, D. S. & Olson, A. J. (2000). *Annu. Rev. Biophys. Biomol. Struct.* **29**, 105–153.
Horjales, E., Altamirano, M. M., Calcagno, M. L., Garratt, R. C. & Oliva, G. (1999). *Structure*, **7**, 527–536.
Jencks, W. P. (1997). *Annu. Rev. Biochem.* **66**, 1–18.
Ji, X., Braxenthaler, M., Moult, J., Fonticelli, C., Bucci, E. & Gilliland, G. L. (1998). *Proteins Struct. Funct. Genet.* **30**, 309–320.
Kidera, A. & Go, N. (1992). *J. Mol. Biol.* **225**, 457–475.
Kimmel, J. L. & Reinhart, G. D. (2000). *Proc. Natl Acad. Sci. USA*, **97**, 3844–3849.
Koshland, D. E. Jr, Nemethy, G. & Filmer, D. (1966). *Biochemistry*, **5**, 365–385.
Midelfort, C. & Rose, I. A. (1977). *Biochemistry*, **16**, 1590–1599.
Monod, J., Wyman, J. & Changeux, J.-P. (1965). *J. Mol. Biol.*, **12**, 88–118.
Montero-Morán, G. M., Horjales, E., Calcagno, M. L. & Altamirano, M. M. (1998). *Biochemistry*, **37**, 7844–7849.
Nicholls, A., Bharadwaj, R. & Honig, B. (1993). *Biophys. J.* **64**, A166.
Noat, G., Ricard, J., Borel, M. & Got, C. (1968). *Eur. J. Biochem.* **5**, 55–70.
Oliva, G., Fontes, M. R. M., Garratt, R. C., Altamirano, M. M., Calcagno, M. L. & Horjales, E. (1995). *Structure*, **3**, 1323–1332.
Otwinowski, Z. (1993). *Proceedings of the CCP4 Study Weekend. Data Collection and Processing*, edited by L. Sawyer, N. Isaacs & S. Bailey, pp. 56–62. Warrington: Daresbury Laboratory.
Otwinowski, Z. & Minor, W. (1996). *Methods Enzymol.* **276**, 307–325.
Perella, M. & Di Cera, E. (1998). *J. Biol. Chem.* **274**, 2605–2608.
Perutz, M. F. (1990). *Mechanisms of Cooperativity and Allosteric Regulation in Proteins.* Cambridge University Press.
Plumbridge, J. A. (1990). *J. Bacteriol.* **172**, 2728–2735.
Rath, V. L., Ammirati, M., Danley, D. E., Ekstrom, J. L., Gibbs, E. M., Hynes, T. R., Mathiowetz, A. M., McPherson, R. K., Olson, T. V., Treadway, J. L. & Hoover, D. J. (2000). *Chem. Biol.* **7**, 677–682.
Rubinson, K. A. (1998). *J. Protein Chem.* **17**, 771–787.
Sakash, J. B. & Kantrowitz, E. R. (2000). *J. Mol. Chem.* **37**, 28701–28707.
Sheldrick, G. M. & Schneider, T. R. (1997). *Methods Enzymol.* **277**, 319–343.
Tovar-Mendez, A., Rodríguez-Stres, R., Lopez-Valentin, D. M. & Muñoz-Clares, R. A. (1998). *Biochem. J.* **332**, 633–642.
Valentini, G., Chiarelli, L., Fortin, R., Speranza, M. L., Galizzi, A. & Mattevi, A. (2000). *J. Biol. Chem.* **275**, 18145–18152.
Willemoes, M., Hove-Jensen, B. & Larsen, S. (2000). *J. Biol. Chem.* **275**, 35408–35412.
Yifrach, O. & Horovitz, A. (1995). *Biochemistry*, **34**, 5303–5308.